# INHIBITION OF FLAMES BY IRON PENTACARBONYL*

Marc D. Rumminger,† Dirk Reinelt,‡ Valeri Babushok, and Gregory T. Linteris
Building and Fire Research Laboratory
National Institute of Standards and Technology
Gaithersburg MD 20899, USA

## INTRODUCTION

Researchers in the 1960s discovered that certain metallic compounds are even more effective flame inhibitors than the halogens [1-3]. In particular, iron pentacarbonyl was found to be up to two orders of magnitude more effective at reducing the burning velocity of hydrocarbon-air flames than Br-containing compounds [1,4]. However, the rapid adoption of $CF_3Br$ as a fire suppressant led to a reduction in research on other agents, and the inhibition mechanism of $Fe(CO)_5$ remained undetermined. As part of the search for replacements for $CF_3Br$, the mechanism of $Fe(CO)_5$ is being re-examined.

In previous research [5-8] we have confirmed that $Fe(CO)_5$ is extraordinarily effective, but have also found that its incremental effectiveness decreases rapidly as it is added in higher concentrations. For example, adding 200 ppm of $Fe(CO)_5$ to premixed methane-air flames reduces the burning velocity by nearly 50%, but increasing the concentration beyond 200 ppm does not lead to significant additional reduction. The goal of the present research is to understand both the powerful inhibition at low concentration and the lack of additional effect as more inhibitor is added. A critical part of the research on $Fe(CO)_5$ is to understand iron pentacarbonyl's diminishing effectiveness at high mole fraction in order to avoid similar behavior in future fire suppressants. We also seek to determine the relative effects of homogeneous and heterogeneous chemistry in the $Fe(CO)_5$ inhibition mechanism. If particulates play a key role in the inhibition, then the search for halon alternatives could be directed toward chemicals that produce similar condensed-phase compounds.

Our study of flame inhibition is intended to provide insights into flame suppression. Although the processes have different end points (weakening the flame vs. extinguishing it), the underlying mechanism is similar: the agent reduces the overall reaction rate of the fuel-air mixture. Inhibition can be viewed as the stage of suppression in which the inhibitor weakens the flame, making it more vulnerable to extinction by external factors such as heat loss or fluid-mechanical instability.

Inhibition—and eventually suppression—occurs as the agent reduces the rate of heat release of the flame. For chemically acting agents, the agent interferes with the reactions that consume the fuel and intermediates. Hence, we can study the effect of small agent concentrations on flame chemistry and build chemical kinetic models that describe the effect of the agent on the combustion reactions. By using laboratory-scale premixed and diffusion flames amenable to

---

* Official contribution of the National Institute of Standards and Technology, not subject to copyright in the United States.

† National Research Council/NIST postdoctoral fellow

‡ Currently with BASF Aktiengesellschaft, 67056 Ludwigshafen, Germany.

modeling, we can validate the chemical kinetic model and gain insight into which processes are most important. Later, we can continue to construct and refine the mechanism for higher inhibitor concentrations and for flames and fuels that are more representative of fires. Finally, an understanding of the modes of action of effective agents such as $Fe(CO)_5$ can lead researchers to chemicals that have similar favorable properties, while avoiding characteristics such as diminishing effectiveness at high concentration.

In this paper, results of numerical simulations of one-dimensional premixed flames of methane, oxygen, nitrogen, and iron pentacarbonyl are presented and compared with experimental measurements to provide insight into the inhibition mechanism. Additionally, premixed flames with argon replacing a portion of the nitrogen are used to examine the effect of flame temperature on the inhibition. For diffusion flames, calculated extinction strain rates of counterflow flames are compared with experimental measurements for cases in which the inhibitor is added to the fuel or air stream.

## EXPERIMENTAL APPROACH

The approach in the present research is to determine the effect of $Fe(CO)_5$ on the overall reaction rate of hydrocarbon-air flames. Since this reaction rate is a fundamental parameter affecting the stabilization and fuel consumption rate of fires, the extent to which it is influenced by the agent is a first measure of the agent's potential as a fire suppressant. Although tests on full-scale fires will be required to assure the effectiveness of any agent, laboratory burners have several important benefits. Their simplicity allows rapid assessment of inhibitor performance in many flame conditions and at various concentrations, and the flames are highly reproducible and stable. Finally, in a well-designed laboratory burner, there is little ambiguity about how much agent reaches the flame.

Two methods are used to obtain overall reaction rate information: measurements of the burning velocity of premixed laminar flames, and measurements of the extinction strain rate of counterflow diffusion flames. Experimental results and the experimental arrangements are described in detail in Reference 8. Both methods provide nearly adiabatic flames in which the measured parameter is easily related to the overall reaction rate, allowing straightforward interpretation of the effect of the inhibitor. In addition, both flames are easily modeled with existing computer programs. By using detailed chemical kinetic mechanisms together with full transport calculations, the chemical species profiles throughout the flames are calculated. These results provide great insight into both the chemical and physical mechanisms of the inhibitor. Although techniques such as detailed flame structure measurements provide information about the chemical species at each location in the flame for one particular condition, the present burning velocity and extinction strain rate measurements have the advantage of allowing rapid testing of the effect of the inhibitor over a wider range of conditions.

## MODELING APPROACH

To understand the powerful inhibition of $Fe(CO)_5$, we solve the equations of mass, momentum, and energy conservation using existing numerical models. The detailed chemical kinetics are described by comprehensive mechanisms for methane oxidation and iron-species inhibition. All calculations and experiments describe flames at one atmosphere pressure, with $Fe(CO)_5$ added to reactant streams in concentrations of up to 500 ppm.

One-dimensional freely-propagating premixed flames are simulated using the Sandia flame code ***Premix**** [9], the *Chemkin* subroutines [IO], and the transport property subroutines [11]. The kinetic and thermodynamic data of GRI-Mech 1.2 [12] (32 species and 177 chemical reactions) serves as a basis for describing the methane combustion, with iron species and reactions added as described below.

One-dimensional counterflow diffusion flames are simulated with a numerical code developed by Smooke [13] and a one-carbon mechanism for methane oxidation [14] (17 species and 52 chemical reactions). The somewhat smaller methane mechanism captures the important chemistry of the flame, while reducing the computational time required for calculating the extinction of the counterflow flames.

## INHIBITION MECHANISM

Previous flame inhibition studies of $Fe(CO)_5$ have been outlined [5, 8]. Although the effect of the agent on the mole fraction of OH radical downstream of the reaction zone was noted, and several important intermediate species were detected spectroscopically [4], no detailed mechanism was proposed. In work related to flame inhibition, authors have discussed inhibition mechanisms that involve catalytic removal of H atoms by metal species (atomic, oxide, or hydroxide). In addition, metallic compounds have been studied in high temperature reacting flows for applications such as flame suppression and materials synthesis, and rates for reactions involving gas-phase metallic compounds are available in the literature. **A** compilation of reactions and rates for metals in flames can be found in Reference 15. The present work is an extension of previous work [7] in which a gas-phase inhibition mechanism was developed based largely upon the work of Jensen and Jones [16]. For completeness, the mechanism has now been expanded to include a more comprehensive set of iron-species reactions, a more detailed decomposition route for $Fe(CO)_5$, and a different route for formation of FeO. The dominant inhibition reactions, however, are fundamentally unchanged.

Using information in the literature and reaction analysis, we compiled a list of iron-containing species that could exist at significant concentrations in flames. In the mechanism used here, the $Fe(CO)_5$ decomposition products are $Fe(CO)_4$, $Fe(CO)_3$, $Fe(CO)_2$, FeCO, and **Fe** [17-20], and the intermediates and product species are Fe, FeO, FeOH, $Fe(OH)_2$, Fe(O)OH, $FeO_2$, and FeH. There is little evidence that any other iron compounds can exist at significant concentra-tions for conditions discussed in this paper. For the iron-containing compounds, the thenno-dynamic data are from References 21-23, and the transport properties are estimated. The complete reaction mechanism (12 species and 55 reactions) can be obtained from Reference 24 or by contacting the authors. It should be emphasized that the comprehensive set of additional reactions adopted for the present calculations should be considered only as a starting point. Numerous changes to both the rates and the reactions may be made once a variety of experimental and theoretical data are available for testing the mechanism.

---

* Certain commercial equipment, instruments, or materials are identified in this paper to adequately specify the procedure. Such identification does not imply recommendation or endorsement by the National Institute of Standards and Technology, nor does it imply that the materials or equipment are necessarily the best available for the intended use.

The reaction mechanism consists of three parts: (1) decomposition of $Fe(CO)_5$, (2) conversion of iron atoms to scavenging species, and (3) scavenging of radicals through a homogeneous catalytic reaction cycle [16]. These parts are schematically depicted in Figure 1.

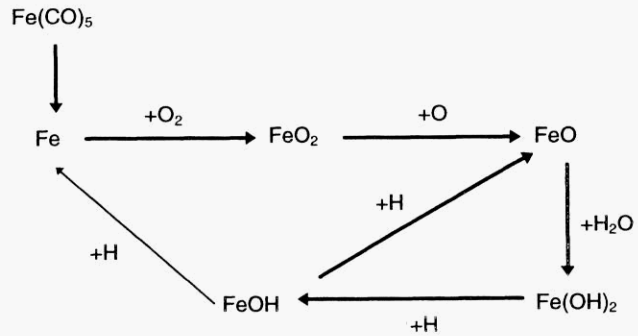


Figure 1. Schematic diagram of reaction pathways based on the gas-phase mechanism described in this paper. Reaction partners are listed next to each arrow.

Our calculations show that the inhibition mechanism is dominated by the catalytic cycle for H-atom recombination

$$FeOH + H \leftrightarrow FeO + H_2 \tag{1}$$

$$FeO + H_2O \leftrightarrow Fe(OH)_2 \tag{2}$$

$$Fe(OH)_2 + H \leftrightarrow FeOH + H_2O \tag{3}$$

$$(\text{net: } H + H \leftrightarrow H_2).$$

The cycle was developed by Jensen and Jones [16] to account for increased rates of hydrogen atom recombination in the products of rich hydrogen-oxygen-nitrogen flames with addition of $Fe(CO)_5$. They obtained rate constants by fitting calculated H-atom concentration profiles to the experimental measurements. Although the rates for the catalytic cycle were derived from a hydrogen-oxygen flame, the sequence is likely to be applicable to a hydrocarbon flame because of the importance of hydrogen-oxygen chemistry in those flames.

## RESULTS AND DISCUSSION

### Premixed Flames

The decrease in the laminar burning velocity is used as a measure of the inhibition action of iron pentacarbonyl. Figure 2 shows the measured (symbols) and calculated (lines) burning velocity of premixed methane-air flames as a function of initial $Fe(CO)_5$ mole fraction ($X_{in}$). For the experiments, the uncertainty in the burning velocity, equivalence ratio, oxygen concentration and $Fe(CO)_5$ mole fraction is ±5%, ±1.4%, ±1.1%, and ±4%, respectively. The figure presents data for three values of the fuel-air equivalence ratio $\phi$. The dotted line shows the calculated burning

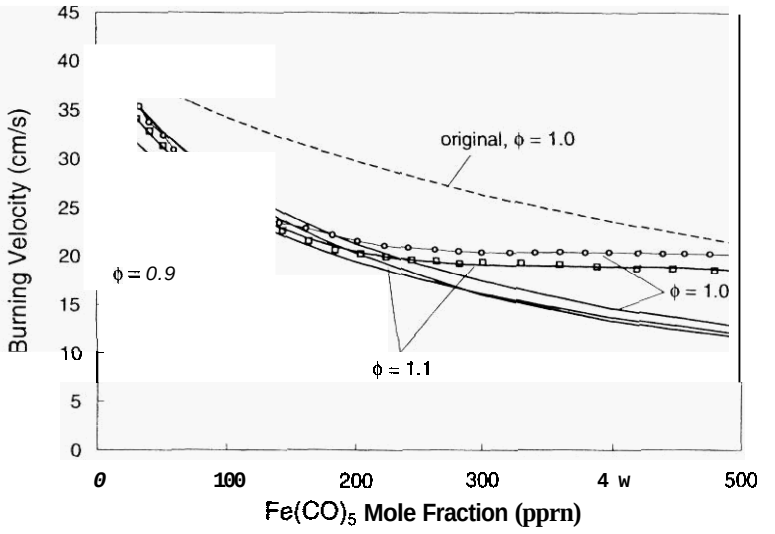


Figure 2. Calculated and measured burning velocity of premixed $CH_4/O_2/N_2$ flames with $X_{O_2,ox} = 0.21$ and varying amounts of $Fe(CO)_5$. The solid lines are the calculated burning velocities using the rates in Reference 24; the dashed line is the calculated burning velocity using the mechanism with the original pre-exponential factors for reactions 1-3 from Reference 16. Symbols are measured normalized burning velocity from Reference **8** for Q0.9 **(A)** $\phi$=1.0 (●) and $\phi$=1.1 (■).

velocity when using the original rates recommended by Jensen and Jones for reactions 1-3 [16]. These calculations are in qualitative agreement with the measurements, but the predicted inhibition is weaker. Sensitivity analysis and numerical experiments show that the burning rate **is** insensitive to both the decomposition rate of $Fe(CO)_5$ and the reaction pathway for Fe conversion to FeO. The burning rate ***is*** sensitive to each reaction in the catalytic cycle (reactions 1-3), roughly equally.

Increasing the pre-exponential term of the specific reaction rate constant by the reported uncertainties (3X, 5X, and 3X for the three reactions, respectively) increases the inhibition effect and leads to better quantitative agreement with the measurements at $\phi$=1.0 and $X_{O_2,ox}$=0.21 ($X_{O_2,ox}$ refers to the oxygen mole fraction in the oxidizer prior to mixing with the fuel). Calculated results with these higher reaction rates are shown as solid lines in Figure **2** (for **the** remainder of the present analyses and figures, these higher values of the pre-exponential term are used.) Such modifications to the mechanism lead to reaction rates that are nearly gas kinetic. Some justification for the use of higher rates exists because of the possibility of condensation of iron species in the experiments of Reference 16, and because the rates are only modified within the reported uncertainty. Nonetheless, it should be emphasized that Jensen and Jones' rate constants were deduced based on measurements in the recombination region of hydrogen-oxygen-nitrogen flames, whereas the present flames are methane-oxygen-nitrogen. Differences in the overall catalytic recombination rates caused by the iron species may be due to additional reactions in the present hydrocarbon system.

Two important features of the inhibition by $Fe(CO)_5$ are captured by the calculations: the strong initial inhibition, and the decrease in the incremental effect of $Fe(CO)_5$ for concentrations above 100 ppm. The experiments, however, show a more abrupt decrease in the inhibition effectiveness at higher $Fe(CO)_5$ mole fractions than do the calculations. Interrogation of the numerical modeling results reveals that the strong inhibition at low mole fraction is due to the early formation of the intermediate species in Reactions 1-3, and the rapid progress of these reactions. For the decrease in effectiveness as the concentration of $Fe(CO)_5$ increases, the model shows that as the inhibition cycle acts to recombine radicals, but that as fewer radicals exist to recombine, the effectiveness decreases, as described below.

In the reaction zone of premixed flames, hydrogen atom is typically present in superequilibrium concentrations. The decrease in the calculated inhibition effect as $X_{in}$ increases is due to the decrease in the quantity of superequilibrium H atoms (defined as the *difference* between the peak $X_H$ in the flame and the equilibrium $X_H$ at the flame temperature) [7, 8, 25, 26]. This decrease can be seen in Figure 3, in which $X_{H,peak} - X_{H,eq}$ is plotted for varying $X_{in}$ as determined from the calculations for the $\phi$=1.0 flame, and a saturation effect is apparent. Interestingly, halogenated flame inhibitors also show a saturation effect [27, 28], and this cause of the reduced effectiveness (reduction in radical superequilibrium) may be the same.

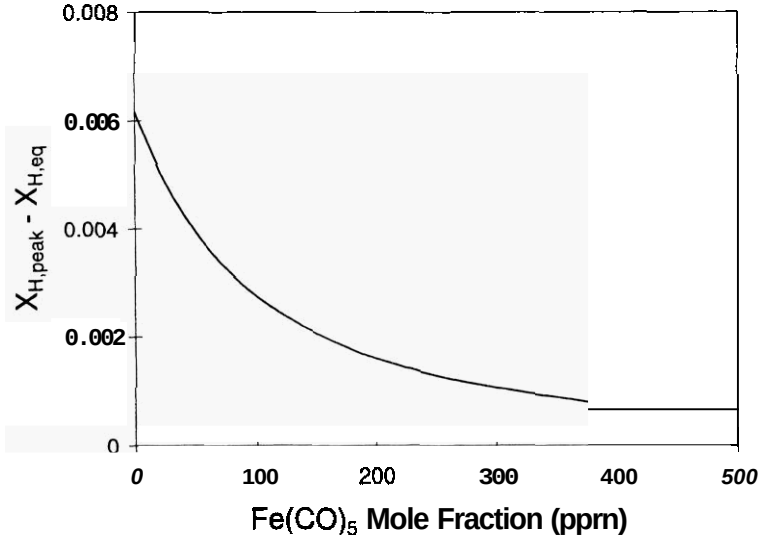


Figure 3. Calculated dependence of superequilibrium H-atom mole fraction ($X_{H,peak} - X_{H,eq}$) on $Fe(CO)_5$ addition in premixed stoichiometric flames with $X_{O_2,ox}$ = 0.21. The calculated value of $X_{H,eq}$ is approximately $2.8 \cdot 10^{-4}$ (for $X_{in} = 0$).

The effect of oxygen mole fraction on the burning velocity is presented in Figure 4, which shows the normalized burning velocity as a function of $X_{in}$ for $\phi$=1.0 flames with three oxidizer compositions: $X_{O_2,ox}$ = 0.20, 0.21, and 0.24 (results for $\phi$ = 1.1, and 0.9 are qualitatively similar). The *normalized* burning velocity is defined as the burning velocity of the inhibited flame divided by the burning velocity of the uninhibited flame (which can be found in Table 1). The experimental results show that as $X_{O_2,ox}$ increases, the inhibition effect at low mole fraction (i.e., the slope) decreases. As Figure 4 illustrates, the numerical model qualitatively predicts this

Table 1. Calculated ($v_{o,num}$) burning velocities, measured ($v_{o,exp}$) burning velocities, and calculated maximum temperatures ($T_{max,num}$) for the uninhibited premixed flames. Data for flames without argon are from Reference 8.

| $\phi$ | $X_{O_2,ox}$ | $\frac{X_{Ar}}{X_{Ar}+X_{N_2}}$ | $v_{o,num}$ (cm/s) | $v_{o,exp}$ (cm/s) | $T_{max,num}$ (K) |
|---|---|---|---|---|---|
| 0.9 | 0.21 | 0 | 36.5 | 37.1 ± 1.9 | 2130 |
| 1.0 | 0.20 | 0 | 35.8 | 33.2 ± 1.7 | 2180 |
| 1.0 | 0.21 | 0 | 40.6 | 45.4 ± 1.4 | 2230 |
| 1.0 | 0.24 | 0 | 55.6 | 59.2 ± 3.0 | 2350 |
| 1.1 | 0.21 | 0 | 40.7 | 39.3 ± 2.0 | 2210 |
| 1.1 | 0.21 | 0.424 | 53.2 | 58.5 ± 3.2 | 2350 |
| 1.1 | 0.21 | 0.63 | 60.7 | 68.1 ± 3.9 | 2420 |

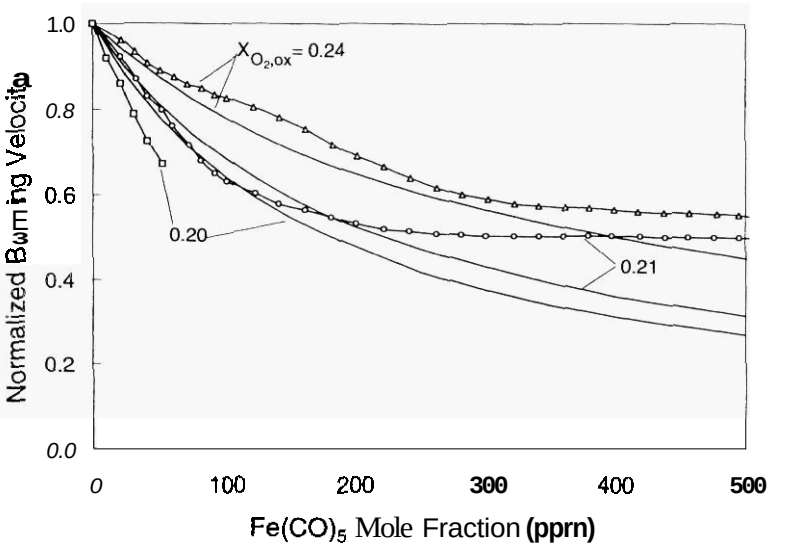


Figure 4. Calculations and measurements of normalized burning velocity of premixed $CH_4/O_2/N_2$ flames with $X_{O_2,ox}$ = 0.20 (■), 0.21 (●), and 0.24 (▲). $\phi$ = 1.0. Experimental data are from Reference 8.

behavior. Examination of the numerical results shows that for stoichiometric flames with 50 ppm $Fe(CO)_5$ in the reactants, the catalytic recombination mechanism accounts for 20, 19, and 15% of the total H-atom reaction flux for consumption of H, for $X_{O_2,ox}$=0.20, 0.21, and 0.24.

That is, at higher oxygen mole fractions, the creation and destruction fluxes for hydrogen become larger, and the iron-species reactions become a smaller fraction of the total flux (for a fixed initial inhibitor mole fraction).

**As** Figure 2 and Figure 4 illustrate, the experiments show a much greater decrease in the effectiveness of $Fe(CO)_5$ as the mole fraction increases than the calculations predict. One possible explanation for this discrepancy is that as the mole fraction of inhibitor increases, there is a loss of the radical-scavenging iron species that is not yet accounted for in the kinetic mechanism. Since the iron species exist in mole fractions above their vapor pressure [7, 24], it is possible that condensation of iron species represents a loss mechanism that is not accounted for

in the calculations. This explanation is consistent with the shift in the value of $X_i$, where the diminished effectiveness occurs in the experiments as shown in Figure **4.** That is, at higher temperatures, there will be a higher vapor pressure for condensed iron species, so the drop-off in effectiveness will not occur until higher $Fe(CO)_5$ mole fractions are reached. Unfortunately, varying the oxygen mole fraction in Figure **4** changes the temperature ***and*** the mole fraction of oxygen-containing species in the flame, both **of** which can change the condensation properties.

In premixed methane-oxygen-diluent flames it is possible to vary the flame temperature without varying $\phi$ and $X_{O_2,ox}$ by changing the composition of the diluent. In this case, we replace nitrogen with argon, thus causing the flame temperature to increase. Figure **5** shows the measured and calculated normalized burning velocity of methane flames at $X_{O_2,ox}$=0.21 and $\phi$=1.1 for final calculated temperatures of **2230,2350,** and **2420 K.** Two results stand out. **As** the gas temperature increases, (1) the inhibition is weaker, and **(2)** the point at which the normalized burning velocity levels off shifts to a higher value of $X_{in}$ **.** The stronger inhibition at lower temperature is a result of a decrease in the quantity of superequilibrium H atoms as described above. The change in leveling-off point may be due to higher vapor pressure of the iron compounds at higher temperature (as discussed **[24]).**

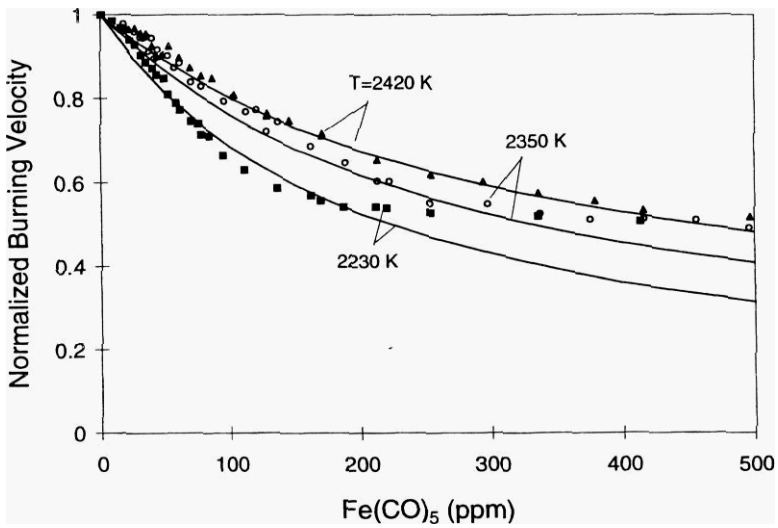


Figure ***5.*** Calculations (lines) and measurements (symbols) of normalized burning velocity of premixed $CH_4/O_2/N_2/Ar$ flames with temperatures **of 2230 K** (no Ar, ■), **2350 K (42.4%** of $N_2$ replaced with Ar, ●), and **2420** K **(63% of** $N_2$ replaced with Ar, **A).** $\phi$= 1.1 and $X_{O_2,ox}$ **= 0.21.**

## COUNTERFLOW DIFFUSION FLAMES

Counterflow diffusion flames provide additional opportunities to study the behavior of $Fe(CO)_5$. The inhibitor can be subjected to different chemical and thermal histories by varying the reactants, the location of the inhibitor addition, and the flame location. The reduction in the extinction strain rate ($a_{ext}$, defined as the axial velocity gradient in the oxidizer stream at extinction) is used as a measure of the inhibition action of iron pentacarbonyl.

The counterflow diffusion flame results are presented in terms of a normalized extinction strain rate, which is defined as the ratio of the extinction strain rate of an inhibited flame to that of an uninhibited flame. The normalized value is used since Chelliah et al. [29] have shown that the absolute values of $a$ can depend on experimental burner design and the numerical description of the flow field, whereas the trends in $a_{ext}$ are independent of the flow-field characteristics in the experiment or model.

Figure **6** shows the measured and calculated normalized extinction strain rates for a methane-air flame with varying $Fe(CO)_5$ input. The flame is located on the oxidizer side of the stagnation plane, and the maximum temperature is approximately 1800 K at extinction. For the uninhibited flame, the measured $a_{ext}$ is $610 \pm 30\ s^{-1}$ and the calculated $a_{ext}$ is $520\ s^{-1}$. Experimental results [8] show that when $Fe(CO)_5$ is added to the oxidizer stream a significant decrease in $a_{ext}$ results. In contrast, when the $Fe(CO)_5$ **is** added to the fuel stream, little change in $a_{ext}$ results. The numerical simulations qualitatively reproduce the significant dependence of inhibition on the location of $Fe(CO)_5$ addition.

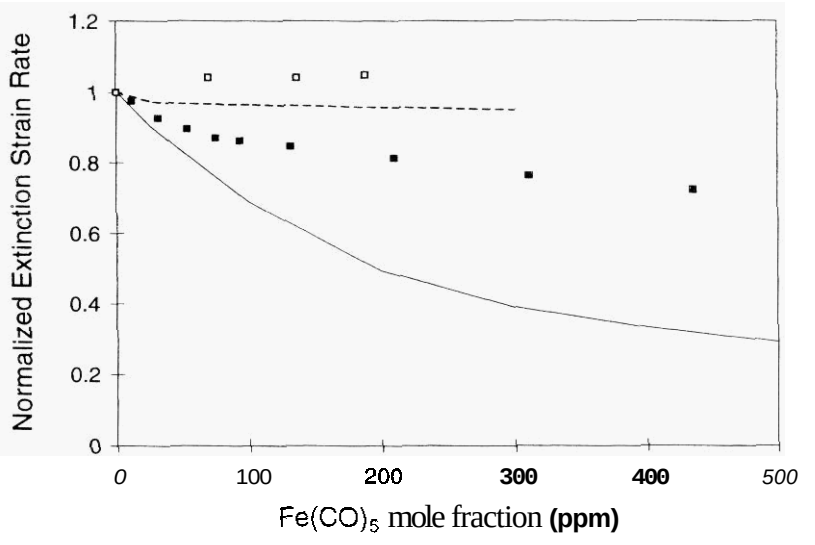


Figure **6.** Normalized extinction strain rate **for** counterflow diffusion flame as $Fe(CO)_5$ input varies. Closed symbols: measurements with the $Fe(CO)_5$ in the oxidizer; open symbols: measurements with $Fe(CO)_5$ in the fuel; solid line: calculations with $Fe(CO)_5$ in the oxidizer; and dashed line: calculation with $Fe(CO)_5$ in the fuel. Experimental data are from Reference 8.

## CONCLUSIONS

While the highly efficient inhibition action of metallic compounds in hydrocarbon-air flames has been known for some time, there has existed controversy in the literature as to whether the mechanism involves gas-phase or heterogeneous chemistry. This paper presents numerical modeling of iron pentacarbonyl's extremely strong inhibition action in Bunsen-type premixed and counterflow diffusion flames, and provides evidence that inhibition occurs primarily by homogeneous gas-phase chemistry at low initial $Fe(CO)_5$ mole fraction. While we do not believe

that the present calculations explicitly rule out heterogeneous chemical effects, we believe that the mechanism, based on homogeneous chemistry, can explain many—but not all—of our measurements.

Calculations using the rate constants for the catalytic cycle reactions (1-3) suggested in Reference 16 yield normalized burning velocities in qualitative agreement with experimental measurements; however, they predict less inhibition than was measured. Analysis of the numerical results confirms that the primary inhibition occurs through the catalytic cycle of reactions (1-3). An increase in the rate constants (within experimental uncertainty) of these reactions leads to improved agreement between experiments and calculations at low $Fe(CO)_5$ mole fractions for several equivalence ratios and oxygen concentrations. At higher initial $Fe(CO)_5$ mole fractions, however, the calculations predict a stronger effect than measured and do not predict as severe a leveling off in burning velocity. Likewise, for a counterflow diffusion flame of methane flowing against air, calculations of the extinction strain rate agree with experimental measurements at low values of $X_{in}$, but at higher $X_{in}$ the simulations predict a stronger effect on $a_{ext}$ than was measured.

The performance of the present gas-phase mechanism is considered very good, and it provides evidence that the flame inhibition effect of $Fe(CO)_5$ is primarily a result of gas-phase scavenging reactions. Nonetheless, certain experimental observations are not fully accounted for. In particular, the predicted inhibition for lean premixed flames is not strong enough. The range of flame temperature studied here is fairly narrow: about 2100 K to 2400 K in the premixed flames and about 1800 K to 2000 K in the diffusion flames. Future research will examine a wider variety of counterflow diffusion flames—which will allow greater variation in temperature and gas composition—and will measure particulate properties to elucidate the role of condensed iron compounds. More research is desirable to test the validity of the higher rates for reactions 1-3 indicated here, and to determine if additional inhibition reactions are important in hydrocarbon flames.

***The financial support of the Alexander von Humboldt Foundation for D.R. and of the Army Research Laboratory (K. McNesby and A. Miziolek) for V.B. is gratefully acknowledged. The helpful suggestions of Professor Harsha Chelliah concerning the counterflow diffusion flame calculations contributed greatly to this research, as did the generosity of Professor Mitchell Smooke for the use of his diffusion flame code. The authors also thank Mr. Newton Liu for helping with the numerical simulations and Dr. Wing Tsang for helpful discussions and suggestions.***

## REFERENCES

1. Lask, G., and Wagner, H.G., ***Eighth Symposium (International) on Combustion,*** Williams and Wilkins Co., Baltimore, MD, 1962, pp. 432-438.
2. Vanpee, M., and Shirodkar, P., ***Seventeenth Symposium (International) on Combustion,*** The Combustion Institute, Pittsburgh, PA, 1979, pp. 787-795.
3. Miller, D.R., Evers, R.L., and Skinner, G.B., ***Combust. Flume*** 7:137 (1963).
4. Bonne, U., Jost, W., and Wagner, H.G., ***Fire Res. Abstracts Rev.*** 4 6 (1962).
5. Reinelt, D. and Linteris, G.T., "Experimental Study of the Flame Inhibition Effect of Iron Pentacarbonyl," "Experimental Study of the Flame Inhibition Effect of Iron Pentacarbonyl," ***Proceedings of the Halon Options Technical Working Conference,*** 7-9 May 1996, Albuquerque, NM.

6. Linteris, G.T., and Reinelt, D., *Conference Proceedings of INTERFLAM '96, Seventh International Fire Science and Engineering Conference,* 26-28 March 1996, Cambridge, England, p. 477.
7. Reinelt, D., Babushok, V., and Linteris, G.T., "Numerical Study of the Inhibition of Premixed and Diffusion Flames by Iron Pentacarbonyl," Eastern States Section Meeting of The Combustion Institute, Hilton Head, SC, December 1996.
8. Reinelt, D., and Linteris, G.T., "Experimental Study of the Inhibition of Premixed and Diffusion Flames by Iron Pentacarbonyl," *26th Symposium (International) on Combustion,* The Combustion Institute, Pittsburgh, PA, 1996, p. **1421.**
9. Kee, R.J., Grcar, J.F., Smooke, M.D., and Miller, J.A., *A Fortran Computer Program for Modeling Steady Laminar One-dimensional Premixed Flames,* Sandia National Laboratories Report SAND85-8240, 1991.
10. Kee, R.J. Rupley, F.M., and Miller, J.A., *CHEMKIN-11: A Fortran Chemical Kinetics Package for the Analysis of Gas Phase Chemical Kinetics,* Sandia National Laboratories, SAND89-8009B, 1989.
11. Kee, R.J., Dixon-Lewis, G., Wamatz, J., Coltrin, R.E, and Miller, J.A., *A Fortran Computer Package for the Evaluation of Gas-Phase, Multicomponent Transport Properties,* Sandia National Laboratories, SAND86-8246, 1986.
12. Frenklach, M., Wang, H., Yu, C.-L., Goldenberg, M., Bowman, C.T., Hanson, R.K., Davidson, D.F., Chang, E.J., Smith, G.P., Golden, D.M., Gardiner, W.C., and Lissianski, V., *GRI-Mech* 1.2, http://www.me.berkeley.edu/gri_mech; and Frenklach, M., Wang, H., Yu, C.-L., Goldenberg, M., Bowman, C.T., Hanson, R.K., Davidson, D.F., Chang, E.J., Smith, G.P., Golden, D.M., Gardiner, W.C., and Lissianski, V. (1995). *GRI-Mech—An Optimized Detailed Chemical Reaction Mechanism for Methane Combustion.* Gas Research Institute Topical Report. No. GRI-95/0058. Chicago, IL.
13. Smooke, M.D., Puri, I.K., and Seshadri, K., *Twenty-First Symposium (International) on Combustion,* The Combustion Institute, Pittsburgh, PA, 1986, p. 1783.
14. Peters, N. and Rogg, B. (Eds.), "Reduced Kinetic Mechanisms for Applications in Combustion Systems," Lecture Notes in Physics, m15, Springer-Verlag, New York, NY, 1993.
15. Jensen, D.E. and Jones, G.A., "Reaction Rate Coefficients for Flame Calculations," *Combust. Flame* **32:**1 (1978).
16. Jensen, D.E. and Jones, G.A., "Catalysis of Radical Recombination in Flames by Iron," *J. Chem. Phys.* 60:3421 (1974).
17. Seder, T.A., Ouderkirk, A.J., Weitz, E., "The Wavelength Dependence of Excimer Laser Photolysis of Fe(CO)5 in the Gas Phase. Transient Infrared Spectroscopy and kinetics of the Fe(CO)x (x=4,3,2) photofragments.," *J. Chem. Phys.* 85(4): 1977 (1986).
18. Engelking, P.C., and Lineberger, W.C., "Laser Photoelectron Spectrometry of the Negative Ions of Iron and Iron Carbonyls. Electron Affinity Determination for the Series Fe(CO)n, n=0,1,2,3,4.," *J. Am. Chem. Soc.* 101(19):5569 (1979).
19. Lewis, K.E., Golden, D.M., and Smith, G.P., "Organometallic Bond Dissociation Energies: Laser Pyrolysis of Fe(CO)5, Cr(CO)6, Mo(CO)6, and W(CO)6," *J. Am. Chem. Soc.* 106:3905 (1984).
20. Weitz, E., "Studies of Coordinatively Unsaturated Metal Carbonyls in the Gas Phase by Transient Infrared Spectroscopy.," *J. Phys. Chem.* 91:3945 (1987).
21. *Gmelin Handbook of Inorganic and Organometallic Chemistry (8th Edition). Fe.* Supplement Vol. B1, Springer-Verlag, New York, NY, 1991, p. 46.

22. Gurvich, L.V., Veyts, I.V., Alcock, C.B. (Eds.), ***Thermodynamic Properties of Individual Substances,*** 3rd Edition, Nauka, Moscow, 1978-1982. (NIST Special Database 5. IVTANTERMO-PC, NIST, Gaithersburg, MD 20899).
23. Chase, M.W., Jr.; Davies, C.A.; Downey, J.R., Jr.; Frurip, D.J.; McDonald, R.A.; Syverud, A.N., ***JANAF Thermochemical Tables*** (Third Edition), ***J. Phys. Chem. Re$ Data,*** Suppl. 1, 1985, 14, 1-1856.
24. Rumminger, M.D., Reinelt, D., Babushok, V., and Linteris, G.T., "Numerical Study of the Inhibition of Premixed And Diffusion Flames by Iron Pentacarbonyl," accepted **for** publication in ***Combustion and Flame,*** February 1998.
25. Hastie, J.W., ***High Temperature Vapors,*** Academic Press, New York, NY, 1975.
26. Biordi, **J.C.,** Lazzara, C.P., Papp, **J.F.,** in ***Halogenated Fire Suppressants*** (R.G. Gann, Ed.), American Chemical Society, Washington, DC, 1975, **p.** 256.
27. Linteris, G.T., and Truett, **L.,** ***Combust. Flame*** 101:15 (1996).
28. Linteris, G.T., Burgess, D.R., Babushok, **V.,** Zachariah, M., Westmoreland, P., and Tsang, W., "Inhibition of Premixed Methane-Air Flames by Fluoroethanes and Fluoropropanes," ***Combust. Flame*** 113(1-2):164 (1998).
29. Chelliah, H.K., Law, C.K., Ueda, T., Smooke, M.D., and Williams, F.A., ***Twenty-Third Symposium (International)*** *on* ***Combustion,*** The Combustion Institute, Pittsburgh, PA, 1991, **p.** 503.